High-Gain Harmonic-Generation Free-Electron Laser Seeded by Harmonics Generated in Gas

M. Labat,[1,9] M. Bellaveglia,[2] M. Bougeard,[11] B. Carré,[11] F. Ciocci,[1] E. Chiadroni,[2] A. Cianchi,[8,2] M. E. Couprie,[9] L. Cultrera,[2] M. Del Franco,[1] G. Di Pirro,[2] A. Drago,[2] M. Ferrario,[2] D. Filippetto,[2] F. Frassetto,[6] A. Gallo,[2] D. Garzella,[11] G. Gatti,[2] L. Giannessi,[1,*] G. Lambert,[12] A. Mostacci,[5] A. Petralia,[1] V. Petrillo,[3,4] L. Poletto,[6] M. Quattromini,[1] J. V. Rau,[7] C. Ronsivalle,[1] E. Sabia,[1] M. Serluca,[5] I. Spassovsky,[1] V. Surrenti,[1] C. Vaccarezza,[2] and C. Vicario[10]

[1]*ENEA C.R. Frascati, Via E. Fermi, 45 00044 Frascati, Roma, Italy*
[2]*INFN-LNF, Via E. Fermi, 40 00044 Frascati, Roma, Italy*
[3]*Università degli Studi di Milano, Via Celoria, 16 20133 Milano, Italy*
[4]*INFN-Mi, Via Celoria, 16 20133 Milano, Italy*
[5]*Università La Sapienza, Piazzale Aldo Moro, 1 00185 Roma, Italy*
[6]*CNR-IFN, Via Trasea 7, 35131 Padova, Italy*
[7]*ISM-CNR Via del Fosso del Cavaliere, 100 00133 Roma, Italy*
[8]*Università di Roma Tor Vergata, Via della Ricerca Scientifica, 1 00133 Roma, Italy*
[9]*SOLEIL, L'Orme des Merisiers Saint-Aubin - BP 48 91192 GIF-sur-Yvette, Cedex, France*
[10]*Paul Scherrer Institute, 5232 Villigen, Switzerland*
[11]*DSM/DRECAM/SPCSI, CEA, Saclay F-91191 Gyf sur Yvette, Cedex, France*
[12]*LOA ENSTA, UMR 7639 Palaiseau, France*

(Received 26 July 2011; published 22 November 2011)

The injection of a seed in a free-electron laser (FEL) amplifier reduces the saturation length and improves the longitudinal coherence. A cascaded FEL, operating in the high-gain harmonic-generation regime, allows us to extend the beneficial effects of the seed to shorter wavelengths. We report on the first operation of a high-gain harmonic-generation free-electron laser, seeded with harmonics generated in gas. The third harmonics of a Ti:sapphire laser, generated in a gas cell, has been amplified and up-converted to its second harmonic ($\lambda_{\mathrm{rad}} = 133$ nm) in a FEL cascaded configuration based on a variable number of modulators and radiators. We studied the transition between coherent harmonic generation and superradiant regime, optimizing the laser performances with respect to the number of modulators and radiators.

DOI: 10.1103/PhysRevLett.107.224801 PACS numbers: 41.60.Cr, 41.50.+h, 42.55.Vc

Short wavelength light sources (VUV to hard x-rays) are required to probe matter at extremely small, molecular to atomic, scales. Short pulse duration permits the detection of ultrafast dynamical effects and high intensities to study the nonlinear phenomena [1–5]. While storage rings have been very successful for decades, new candidates have recently emerged, enlarging the range of the possibilities of user applications. Among them, free-electron lasers (FELs) are one of the most performing devices for delivering short and intense pulses characterized by ultra high brilliance in the vacuum ultravolet (VUV) and X-ray regions of the spectrum [6,7]. FEL relies on the interaction between a relativistic electron beam, wiggling in the periodic magnetic field of an undulator, and an electromagnetic (e.m.) radiation. When the e.m. radiation wavelength matches the resonant wavelength of the undulator $\lambda_R = \frac{\lambda_u}{2\gamma^2}(1 + K^2/2)$ (λ_u being the undulator magnetic field period, $K = eB_u\lambda_u/(2\pi m_e c)$ its deflection parameter and γ the Lorentz factor of the electrons), the interaction leads to an energy modulation of the electron bunch, further converted into a density modulation. The microbunching allows the emission of coherent radiation at λ_R and its harmonics λ_R/n. In the self-amplified spontaneous emission (SASE) configuration [8–11], the e.m. radiation is the spontaneous emission of the electrons. SASE FELs can deliver very short wavelengths [6,7,12,13], but suffer a limited temporal coherence [11,14] due to the intrinsic fluctuations of the initial shot noise. In the seeded amplifier configuration [15,16], the optical radiation is an external coherent source, which enables to reach a higher degree of temporal coherence within a shorter distance.

To increase the frequency up-conversion of seeded FELs, the cascaded scheme was proposed [16]. An external seed induces energy modulation with a strong harmonic content in a first undulator, called modulator. The modulated beam propagates into a second undulator, the radiator, which is tuned at one harmonics of the modulator and produces radiation directly at this wavelength. This scheme was successfully demonstrated first in the midinfrared [17], and then in the ultraviolet range [18]. Conventional lasers are, however, basically limited at short wavelengths to the visible or near UV range. For further reducing the cascaded FEL output wavelength, the use of high order harmonics generated in gas (HHG) [19–22] as a seed was suggested [23]. The amplifier configuration was demonstrated at SCSS [24].

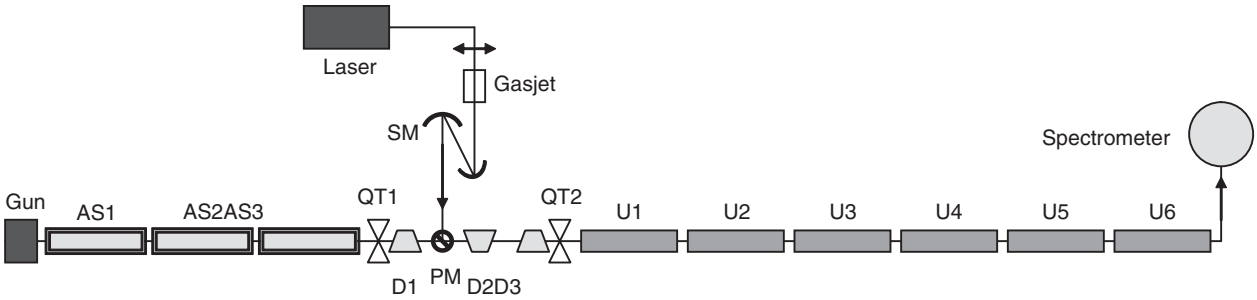

FIG. 1. Schematic of the SPARC layout. Gun: RF photoinjector (SLAC/BNL/UCLA 1.6 cell S-band RF). AS: Accelerating sections. QT: triplet of quadrupoles. D: dipole. U: undulator section. SM: spherical mirrors, PM: periscope mirrors. Spectrometer: normal incidence grating imaging the variable entrance slit on an UV grade CCD camera (Versarray, 1300B-Princeton Instruments).

In this Letter, we present the first operation of a cascaded FEL, seeded with harmonics generated in gas. The FEL was seeded at the third harmonics of the Ti:sapphire ($\lambda_{\text{seed}} = 266$ nm) laser and the radiation at the second harmonics of the seed ($\lambda_{\text{rad}} = 133$ nm) was generated, demonstrating the feasibility of a modulator-radiator FEL scheme, driven by HHG. Because of the low intensity of the seed, the efficient electron beam energy modulation can be reached only after some amplification in the FEL modulator. The dependence of the laser performances on the length of the FEL modulator and radiator sections has been studied. The transition between the coherent harmonic-generation regime, where the beam bunching is generated in the modulator, and the superradiant regime [14,25], where the modulation is self induced by the radiation field at the harmonic wavelength, has been investigated.

The experiments were performed at the UV FEL of the SPARC facility [26], whose basic layout is illustrated in Fig. 1. The electron beam (see Table I) is delivered by a RF photoinjector with a repetition rate of 10 Hz and accelerated in the range of 120–180 MeV. It is then driven via a transfer line to an undulator consisting of six sections of 75 periods each, with a period length of 2.8 cm [27]. The gap of each section can be tuned independently between 8 and 25 mm, so that the undulators may be independently tuned at λ_{seed} as modulator, or at λ_{rad} as radiator.

The laser to generate the seed is based on a regenerative Ti:sapphire amplifier driven by the same oscillator driving the photocatode laser system and delivering up to 2.5 mJ at 800 nm with a pulse duration $\Delta t \sim 120$ fs-FWHM. The infrared laser is focused in an Argon gas cell located in dedicated chambers [28] for the generation of odd nonlinear harmonics up to the 7th order (266, 160, and 114 nm). The harmonic beam is refocused by a pair of spherical mirrors and injected in the undulator by means of a periscope with piezo controlled mirrors for adjusting the transverse alignment. The infrared light generating the seed is not filtered prior to injection in the FEL amplifier. A magnetic chicane deflects the electron beam from the straight path to permit the mirror insertion. The electron-seed temporal overlap is ensured by an optical delay line. Temporal synchronization is achieved by monitoring the spontaneous emission and seed laser signals on a fast photodiode located at the undulators exit. The main output radiation diagnostic is an in-vacuum spectrometer [29], allowing simultaneous single shot measurements of the vertical and spectral distributions and of the absolute pulse energy with an uncertainty due to the transfer function converting the pixel intensity level to an absolute energy of about 30% [26].

TABLE I. Main parameters of the electron beam in two different experimental setups (a) and (b). p: projected. s: slice.

Parameter	(a)	(b)
Bunch Charge (pC)	500 ± 20	300 ± 12
Beam energy E_b (MeV)	176.1 ± 0.2	176.2 ± 0.5
Peak Current I (A)	70 ± 15	50 ± 10
ϵ_x (mm mrad)	2.9 ± 0.15	1.8 ± 0.09
ϵ_y (mm mrad)	3.5 ± 0.18	2.5 ± 0.13
Energy spread (p)	$10 \pm 1 \times 10^{-4}$	$8 \pm 1 \times 10^{-4}$
Energy spread (s)	$5.5 \pm 1 \times 10^{-4}$	$4 \pm 1 \times 10^{-4}$
Length rms (ps)	2.5 ± 0.1	2.2 ± 0.1

With the beam parameters presented in Table I(a), and the undulator tuned at 266 nm as a single amplifier, the SASE FEL does not reach saturation and the output energy is about 12 ± 4 nJ (uncertainties refer to 1 standard deviation over 100 shots). The FEL gain length $L_G = 1.1 \pm 0.2$ m has been estimated by varying the number of effective undulators, progressively detuning the gaps of the last three modules. The Pierce parameter ρ may be derived from the expression $\rho = \lambda_u/(4\pi\sqrt{3}L_G) = 1.1 \times 10^{-3} \pm 2 \times 10^{-4}$. When the FEL amplifier is seeded, the output energy increases up to 2.6 ± 0.76 μJ corresponding to an amplification factor of $\sim$20 (the seed energy at 266 nm, measured at the end of the undulator was 120 ± 26 nJ) and more than 200 times the energy available in the SASE mode. The pulse energy at which the FEL enters saturation is $E_s \sim \rho I \Delta t E_b/e_0 \sim 1.7$ μJ (being e_0 the electron charge), and should be reached, in seeded mode, after the first two undulators. The comparison of the spectra, illustrated in Fig. 2, shows the suppression

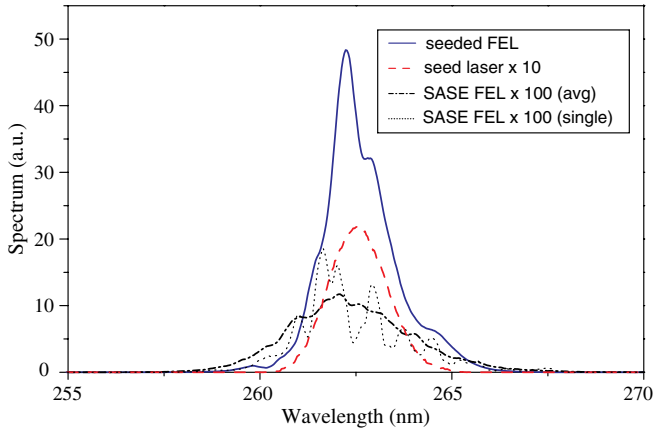

FIG. 2 (color online). Measured spectra of the seed laser, SASE and seeded FEL. The seed spectrum (dashed red line) is multiplied by a factor 10. The SASE spectra in single shot (dotted black line) and averaged over 100 shots (dot-dashed black line) are multiplied by a factor 100. The continuous blue line represents the seeded FEL spectrum averaged over 100 shots. Electron beam parameters are shown in Table I(a).

of the SASE spiky structure and a narrowing of the bandwidth from 3.1 to 1.4 nm-FWHM. The spectrum exhibits an internal structure, with systematic regularities, visible even after the average over 100 events (continuous blue line). This structure (sidebands) is an indication of saturation. Another indication of saturation is nonlinear harmonic generation; while harmonics are not observed in the SASE mode, when injecting the seed, an energy of 500 pJ at the 5th harmonics has been measured. It was not possible to measure the third harmonics because of the low signal to background ratio due to the residual infrared laser, which could be removed by filtering below 70 nm only.

The variable gap undulator allows optimization of the harmonic generation process by configuring the FEL as a cascade, i.e., by tuning the gap of the last sections to the second harmonic of the first one. In this condition, beam matching can be optimized only in a fraction of the whole undulator. Matching is obtained combining the natural undulators vertical focusing with the horizontal focusing of quadrupoles placed in the undulator intersections. A local change of the resonance condition has an impact on the vertical focusing and causes an optical mismatch. Figure 3 shows an example of the optics used in a configuration based on three undulator sections tuned at the fundamental for modulation and on three sections at the second harmonics for radiation (we use the notation $3M/3R$). The quadrupole currents in the second part of the undulator tuned at λ_{rad} have been calculated by minimizing the transverse beam size, while maintaining the transverse symmetry of an expanding beam. The beam optics in configurations tested with four modulators/two radiators ($4M/2R$) and five modulators/one radiator ($5M/1R$) is derived from this one by removing a section at the end and by adding a matched section at the entrance.

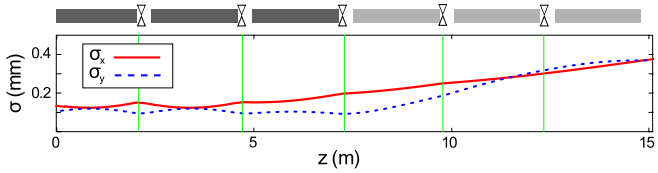

FIG. 3 (color online). Calculated beam transverse dimensions σ_x (solid line) and σ_y (dashed line) vs z along the undulator in the configuration with three modulator sections ($K = 1.59$) and three radiators ($K = 0.507$) ($3M/3R$). The matching is maintained over the first three modulator sections.

With an input seed of 40 ± 10 nJ and the $3M/3R$ configuration, we obtain an energy value $\langle E \rangle = 390 \pm 250$ nJ at 133 nm. Varying the number of modulating sections allows to tune the bunching on the second harmonics at the entrance of the radiators, maximizing the frequency conversion efficiency. The output radiation properties are then studied as a function of the number of sections used for modulation. Energy and relative bandwidth of the sequence of the 100 experimental shots for the three cases are presented in Fig. 4. The energy differences within an order of magnitude, suggest that saturation is always reached in the modulator in the three configurations. The best condition is found with the $4M/2R$ configuration: the mean output energy $\langle E \rangle$ reaches a maximum of 840 ± 270 nJ, with a bandwidth of 0.19%. In the $5M/1R$ configuration, the energy decreases to $\langle E \rangle = 125 \pm 90$ nJ.

In Fig. 5, the comparison between the experimental data and the results of a statistical study made with 100 random shots, simulated by GENESIS 1.3 (red symbols) [30], is shown. The simulated data are in a fairly good agreement with the experiment. The analysis of the simulation data allows a better understanding of the beam dynamics in the different configurations. In Fig. 6, the simulated longitudinal FEL power at the end of the six undulator modules is

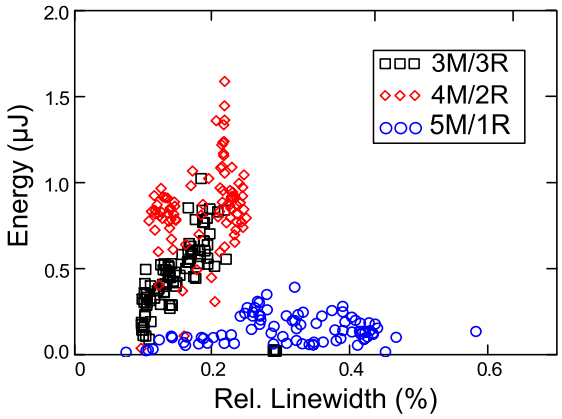

FIG. 4 (color online). Energy (nJ) vs relative linewidth (%) for 100 experimental shots in the configurations: $3M/3R$ (black squares), $4M/2R$ (red diamonds) and $5M/1R$ (blue circles). Electron beam: Table I(b)

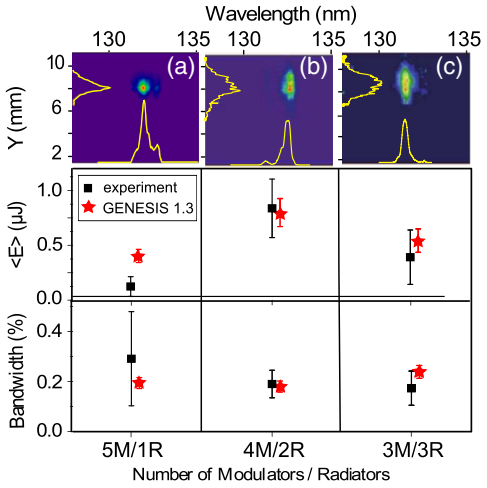

FIG. 5 (color online). Cascaded FEL pulse energy and bandwidth at 133 nm at the end of the undulator in the $5M/1R$, $4M/2R$ and $3M/3R$ configurations; experimental data (black squares) and simulations by GENESIS 1.3 (red stars). Data averaged over 100 shots. Error bars represent ± 1 standard deviation. Electron beam parameter of Table I(b). Seed energy: 40 ± 10 nJ. Simulation data: current $I = 49 \pm 6$ A and beam energy $E = 176.2 \pm 0.35$ MeV [similar to those of Table I(b)], emittance $\epsilon_{x,y} = 0.9 \pm 0.25$ mm mrad (estimate of the slice parameters based on a 80% charge cut) and energy spread $\Delta E/E = 10^{-4} \pm 10^{-5}$ (minimum slice energy spread along the longitudinal bunch coordinate). The images in (a),(b),(c) correspond to single shot spectra acquisitions in the various configurations.

represented. Simulations confirm that in all the configurations the FEL reaches saturation at the end of the modulator. In the $5M/1R$ configuration (a) the deep saturation in the long modulator, results in a very strong bunching with a high harmonic content, enabling the emission of coherent radiation at $\lambda_{\mathrm{rad}} = 133$ nm in the last radiator module. This regime is known as the coherent harmonic generation [31]. The longitudinal pulse structure reveals the overbunching, which occured in the modulator with multiple peaks determined by the particles synchrotron oscillation at 266 nm [32]. In the experiment, we observe a broad spectrum with sidebands and large shot to shot fluctuations [see Fig. 5(a)]. In the $4M/2R$ configuration (b), the radiation at $\lambda_{\mathrm{rad}} = 133$ nm is progressively amplified along the available two radiator modules. In the leading edge of the pulse, a superradiant peak develops, slipping toward the unmodulated electron beam region, which offers a higher gain. The generated output power is higher and the spectrum is narrower, as confirmed by the experiment. The PERSEO simulation, in the $3M/3R$ configuration [Fig. 6(c)], shows a more pronounced build up of the superradiant peak together with a clear modulation at the second harmonic wavelength in the phase space. In the GENESIS 1.3 simulation, and in agreement with the experiment, no further increase of the output power could be observed. This is likely due to the

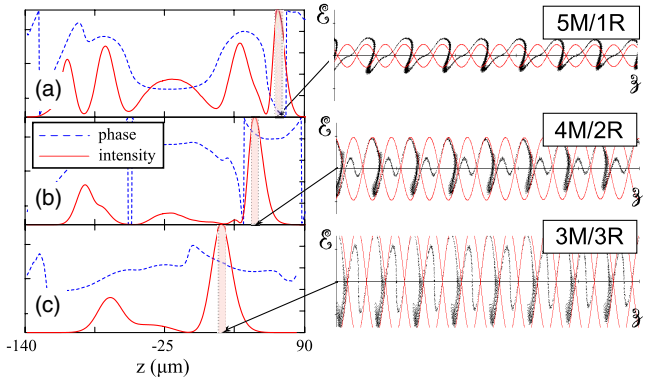

FIG. 6 (color online). Radiation power (solid line, a.u.) and phase profiles (dotted line) on the left side, and e-beam phase space (energy $\mathcal{E}$ vs phase ϑ) in the highlighted region at the end of the six undulator sections, on the right side. (a) Configuration $5M/1R$, (b) $4M/2R$ and (c) $3M/3R$. Simulation with PERSEO [33].

electron beam matching degradation in the last modules in the $3M/3R$ configuration (see Fig. 3), which is not included in the PERSEO model.

In this Letter, we have experimentally demonstrated the feasibility of a cascaded FEL configuration seeded by harmonics generated in gas. Up to about 4×10^{12} photons with high coherence at 133 nm were produced. The transition between the coherent harmonic generation and superradiant emission was investigated, providing insights in novel methods for producing coherent radiation at short wavelengths.

*luca.giannessi@enea.it

[1] J. Miao *et al.*, Proc. Natl. Acad. Sci. U.S.A. **100**, 110 (2003).
[2] H. N. Chapman *et al.*, Nature Phys. **2**, 839 (2006).
[3] K. J. Gaffney and H. N. Chapman, Science **316**, 1444 (2007).
[4] R. Neutze *et al.*, Nature (London) **406**, 752 (2000).
[5] L. Young *et al.*, Nature (London) **466**, 56 (2010).
[6] DESY, Tech. Rep., www.desy.de (2010).
[7] P. Emma *et al.*, Nat. Photon. **4**, 641 (2010).
[8] H. Haus, IEEE J. Quantum Electron. **17**, 1427 (1981).
[9] G. Dattoli, A. Marino, A. Renieri, and F. Romanelli, IEEE J. Quantum Electron. **17**, 1371 (1981).
[10] R. Bonifacio, C. Pellegrini, and L. M. Narducci, Opt. Commun. **50**, 373 (1984).
[11] E. L. Saldin *et al.*, Opt. Commun. **148**, 383 (1998).
[12] R. Brinckman, in *Proceedings of the 2006 FEL Conference, Berlin (DE)*, http://epaper.kek.jp/f06, 2006, p. MOBAU03.
[13] T. Shintake *et al.*, Phys. Rev. ST Accel. Beams **12**, 070701 (2009).
[14] R. Bonifacio *et al.*, Phys. Rev. Lett. **73**, 70 (1994).
[15] I. Boscolo *et al.*, Nuovo Cimento Soc. Ital. Fis. B **58**, 267 (1980).

[16] L. H. Yu, Phys. Rev. A **44**, 5178 (1991).
[17] L. H. Yu *et al.*, Science **289**, 932 (2000).
[18] L. H. Yu *et al.*, Phys. Rev. Lett. **91**, 074801 (2003).
[19] M. Lewenstein *et al.*, Phys. Rev. A **49**, 2117 (1994).
[20] J. Seres *et al.*, Nature (London) **433**, 596 (2005).
[21] M. Ferray *et al.*, J. Phys. B **21**, L31 (1988).
[22] A. McPherson *et al.*, J. Opt. Soc. Am. B **4**, 595 (1987).
[23] D. Garzella *et al.*, Nucl. Instrum. Methods Phys. Res., Sect. A **528**, 502 (2004).
[24] G. Lambert, *et al.*, Nature Phys. **4**, 296 (2008).
[25] L. Giannessi, P. Musumeci, and S. Spampinati, J. Appl. Phys. **98**, 043110 (2005).
[26] L. Giannessi *et al.*, Phys. Rev. ST Accel. Beams **14**, 060712 (2011).
[27] M. Quattromini *et al.*, in *Proceedings of the 2008 EPAC Conference*, www.jacow.org, 2008, p. WEPC124.
[28] O. Tcherbakoff, in *Proceedings of the 2006 EPAC* (Edinburgh, UK, 2006).
[29] L. Poletto *et al.*, Rev. Sci. Instrum. **75**, 4413 (2004).
[30] S. Reiche, Nucl. Instrum. Methods Phys. Res., Sect. A **429**, 243 (1999).
[31] J. Ortega *et al.*, IEEE J. Quantum Electron. **21**, 909 (1985).
[32] M. Labat *et al.*, Phys. Rev. Lett. **103**, 264801 (2009).
[33] L. Giannessi, Phys. Rev. ST Accel. Beams **6**, 114802 (2003).